ARTICLE IN PRESS

+ MODEL

Available online at www.sciencedirect.com

ScienceDirect

Neuropharmacology xx (2008) 1–12

NEURO PHARMACOLOGY

www.elsevier.com/locate/neuropharm

Characterization of aconitine-induced block of delayed rectifier K^+ current in differentiated NG108-15 neuronal cells

Ming-Wei Lin [a], Ya-Jean Wang [a], Shiuh-Inn Liu [b], An-An Lin [c], Yi-Ching Lo [d], Sheng-Nan Wu [a,c,*]

[a] *Institute of Basic Medical Sciences, National Cheng Kung University Medical College, Tainan, Taiwan*
[b] *Department of Surgery, Kaohsiung Veterans General Hospital, Kaohsiung City, Taiwan*
[c] *Department of Physiology, National Cheng Kung University Medical College, Tainan, Taiwan*
[d] *Department of Pharmacology, Kaohsiung Medical University, Kaohsiung, Taiwan*

Received 30 October 2007; received in revised form 21 December 2007; accepted 28 January 2008

Abstract

The effects of aconitine (ACO), a highly toxic alkaloid, on ion currents in differentiated NG108-15 neuronal cells were investigated in this study. ACO (0.3–30 μM) suppressed the amplitude of delayed rectifier K^+ current ($I_{K(DR)}$) in a concentration-dependent manner with an IC_{50} value of 3.1 μM. The presence of ACO enhanced the rate and extent of $I_{K(DR)}$ inactivation, although it had no effect on the initial activation phase of $I_{K(DR)}$. It could shift the inactivation curve of $I_{K(DR)}$ to a hyperpolarized potential with no change in the slope factor. Cumulative inactivation for $I_{K(DR)}$ was also enhanced by ACO. Orphenadrine (30 μM) or methyllycaconitine (30 μM) slightly suppressed $I_{K(DR)}$ without modifying current decay. ACO (10 μM) had an inhibitory effect on voltage-dependent Na^+ current (I_{Na}). Under current-clamp recordings, ACO increased the firing and widening of action potentials in these cells. With the aid of the minimal binding scheme, the ACO actions on $I_{K(DR)}$ was quantitatively provided with a dissociation constant of 0.6 μM. A modeled cell was designed to duplicate its inhibitory effect on spontaneous pacemaking. ACO also blocked $I_{K(DR)}$ in neuroblastoma SH-SY5Y cells. Taken together, the experimental data and simulations show that ACO can block delayed rectifier K^+ channels of neurons in a concentration- and state-dependent manner. Changes in action potentials induced by ACO in neurons *in vivo* can be explained mainly by its blocking actions on $I_{K(DR)}$ and I_{Na}.

Keywords: Aconitine; NG108-15 cells; Delayed rectifier K^+ current; Na^+ current; Action potential

1. Introduction

Aconitine (ACO) is a highly toxic diterpenoid alkaloid occurring in plants of the *Aconitum* genus. ACO and its structurally related analogs are recognized for their phytomedical effects on the heart, central nervous system, and skeletal muscle (Ameri, 1998). The effects on Na^+ channels have thus been demonstrated to underlie toxicological or antinociceptive effects of this compound (Friese et al., 1997; Xu et al., 2006). It was thought that ACO binds with high affinity to the open state of voltage-gated Na^+ channels, thus causing a persistent activation of Na^+ channels by blocking their inactivation (Ameri, 1998; Wang and Wang, 2003; Fu et al., 2006). It has also been demonstrated that the increased amplitude of persistent Na^+ currents by ACO underlies the prolongation of action potentials (Ameri, 1998; Wright, 2001; Amran et al., 2004). Methyllycaconitine, its structurally-related analog, was reported to be effective in antagonizing α_7-nicotinic receptors (Hardick et al., 1995; Ameri, 1998). However, little information is available regarding the actions of ACO-related alkaloids on voltage-gated K^+ channels, although ACO was able to affect the repolarization phase of action potentials.

NG108-15 cells have been used as a neuron model in neurophysiology and pharmacology research (Brown and Higashida, 1988; Meves et al., 1999). It is a hybrid cell line

* Corresponding author. Department of Physiology, National Cheng Kung University Medical College, No. 1, University Road, Tainan 70101, Taiwan. Tel.: +886 6 235 3535x5334; fax: +886 6 236 2780.
E-mail address: snwu@mail.ncku.edu.tw (S.-N. Wu).

0028-3908/$ - see front matter © 2008 Elsevier Ltd. All rights reserved.
doi:10.1016/j.neuropharm.2008.01.009

derived from the fusion of two separate cell lines, mouse neuroblastoma (N18TG-2, a subclone of mouse C1300 neuroblastoma cells) and rat glioma (C6BV-1, a subclone of rat C6 glioma) (Brown and Higashida, 1988). This cell line was reported to express Kv3.1a mRNA and to exhibit the activity of delayed rectifier K^+ (K_{DR}) channels (Brown and Higashida, 1988; Yokoyama et al., 1989; Wu et al., 2001; Lo et al., 2003). In addition, the expression levels of $Na_v1.7$ were elevated in NG108-15 cells when neuronal differentiation was induced by pretreatment with a cyclic AMP analogue (Kawaguchi et al., 2007).

A characteristic feature of delayed rectification for K^+ channels (i.e., K_{DR} channels) is that brief depolarization activates the channel, but sustained depolarization can produce a slow inactivation (Baukrowitz and Yellen, 1995; Rasmusson et al., 1998; Fernandez et al., 2003). Inactivation is a basic conformational change intrinsic to most of the K^+ channels that controls repolarization. Inactivation has been observed for many cloned K^+ channels of the Kv superfamily, and is generally termed ''C-type inactivation'', to be distinguished from ''N-type'' inactivation by the ''ball-and-chain'' mechanism (Baukrowitz and Yellen, 1995; Rasmusson et al., 1998). K_{DR} channels with slow inactivation have been reported to affect the fluctuation in resting membrane potential (Marom, 1998). Moreover, the role of K_{DR} channels, particularly members of the Kv3 superfamily present in time-coding neurons is to stabilize the resting membrane potential and effectively reduce the broadening of high-frequency action potentials (Hernandez-Pineda et al., 1999; Rudy and McBain, 2001; Lien and Jonas, 2003; Tateno and Robinson, 2007). A similar type of inactivation has been characterized in Kv3.1 channels (Marom et al., 1993; Klemic et al., 2001).

Therefore, the objective of this study is to determine whether ACO, a highly potent neurotoxin, has any effects on ion currents and membrane potential in differentiated NG108-15 neuronal cells. Of note, we found that in these cells, in addition to inhibition of voltage-gated Na^+ current (I_{Na}), ACO could produce inhibitory effects on delayed rectifier K^+ current ($I_{K(DR)}$) in a concentration- and state-dependent fashion. Current inactivation of $I_{K(DR)}$ in the presence of ACO was also quantitatively characterized. Similar effects were also observed in neuroblastoma SH-SY5Y cells. The major action of ACO on $I_{K(DR)}$ is thought to be through an open-channel mechanism. Simulation studies can also duplicate experimental results.

2. Materials and methods

2.1. Cell preparation and differentiation

The clonal strain NG108-15 cell line, formed by Sendai virus-induced fusion of the mouse neuroblastoma clone N18TG-2 and the rat glioma clone Cg BV-1, was originally obtained from the European Collection of Cell Cultures (ECACC-88112302; Wiltshire, UK). NG108-15 cells were kept in monolayer cultures at a density of 10^6/ml in plastic disks containing Dulbecco's modified Eagle's medium (DMEM; Life Technologies, Gaithersburg, MD, USA) supplemented with 100 μM hypoxanthine, 1 μM aminopterin, 16 μM thymidine, and 5% (w/v) fetal bovine serum (FBS) as the culture medium, in a humidified incubator equilibrated with 90% O_2/10% CO_2 at 37 °C (Wu et al., 2001). The experiments were generally performed after 5 days of subcultivation (60–80% confluence). To induce neuronal differentiation, culture medium was replaced with medium containing 1 mM dibutyryl cyclic-AMP and cells were cultured in the incubator for 1–7 days. NG108-15 cells proliferated well in the culture medium; however, they stopped proliferating and showed the growth of neurites in response to dibutyryl cyclic-AMP (Tojima et al., 2003). The numbers of neurites and varicosities were found to be significantly increased in NG108-15 cells treated with 1 mM dibutyryl cyclic AMP.

Human neuroblastoma SH-SY5Y cells were obtained from American Type Culture Collection ([CRL-2266]; Manassas, VA, USA). Cells were maintained in DMEM supplemented with 10% FBS, penicillin (200 U/ml), and streptomycin (100 μg/ml) in an incubator at 37 °C, containing 5% CO_2. To induce differentiation, SH-SY5Y cells were treated with all-*trans* retinoic acid (10 μM) and 2% fetal calf serum for 5–7 days before the experiments were made.

2.2. Electrophysiological measurements

Cells used for electrophysiological experiments were dissociated and an aliquot of cell suspension was transferred to a recording chamber mounted on the stage of an inverted DM-IL microscope (Leica Microsystems, Wetzlar, Germany). Cells were bathed at room temperature (20–25 °C) in normal Tyrode's solution containing 1.8 mM $CaCl_2$. Patch pipettes were pulled from Kimax-51 glass capillaries (1.5–1.8 mm o.d., Kimble; Vineland, NJ, USA) using a two-stage electrode puller (PP-830, Narishige, Tokyo, Japan) and the tips fire-polished with a microforge (MF-83; Narishige). Pipettes used had a resistance of 3–5 MΩ when immersed in normal Tyrode's solution. Ion currents were measured with glass pipettes in the whole-cell configuration of the patch-clamp technique, using an RK-400 (Biologic, Claix, France) or an Axopatch 200B patch-clamp amplifier (Molecular Devices, Sunnyvale, CA, USA) (Wu et al., 2001).

2.3. Data recording and analyses

The signals were displayed on an analog/digital oscilloscope (HM-507; Hameg, East Meadow, NY, USA) and on a Dell 2407WFP-HC LCD monitor (Round Rock, TX, USA). The data were stored online in a Slimnote VX_3 computer (Lemel, Taipei, Taiwan) at 10 kHz through a Digidata-1322A interface (Molecular Devices). This device was controlled by pCLAMP 9.0 software (Molecular Devices). Currents were low-pass filtered at 1 or 3 kHz. Ion currents recorded during whole-cell experiments were digitally stored and analyzed subsequently by use of pCLAMP 9.0 (Molecular Devices), Origin 7.5 software (OriginLab, Northampton, MA, USA), SigmaPlot 7.0 software (SPSS, Apex, NC, USA), or custom-made macros in Microsoft Excel (Redmont, WA, USA). The pCLAMP-generated voltage-step protocols were generally used to measure the current-voltage (I–V) relations for ion currents (e.g., I_{Na} or $I_{K(DR)}$). Action potential duration was measured at 50% of repolarization.

The concentration-response data for inhibition of $I_{K(DR)}$ were fitted to the Hill equation:

$$\text{Percentage inhibition} = \frac{E_{max} + [C]^n}{[C]^n + IC_{50}^n},$$

where $[C]$ represents the concentration of ACO; and IC_{50} and n are the concentration required for a 50% inhibition and Hill coefficient, respectively; and E_{max} is ACO-induced maximal inhibition of $I_{K(DR)}$. Microsoft Solver in Excel was generally used to fit data by a least-squares algorithm.

Values were provided as means ± SEM with sample sizes (n) indicating the number of cells from which the data were obtained. The paired or unpaired Student's t-test and one-way analysis of variance with the least-significance-difference method for multiple comparisons were used for the statistical evaluation of differences among means. Statistical significance was determined at a P value of <0.05.

2.4. Drugs and solutions

ACO (aconitine or acetylbenzoylaconine, $C_{34}H_{47}NO_{11}$), dibutyryl cyclic AMP, orphenadrine citrate, tetraethylammonium chloride, tetrodotoxin,

Please cite this article in press as: Lin, M.-W. et al., Characterization of aconitine-induced block of delayed rectifier K^+ current in differentiated NG108-15 neuronal cells, Neuropharmacology (2008), doi:10.1016/j.neuropharm.2008.01.009

all-*trans* retinoic acid and tetrodotoxin were purchased from Sigma Chemicals (St. Louis, MO, USA). The purity of ACO was over 99%. Methyllycaconitine was obtained from Tocris (Bristol, UK), 5-hydroxydecanoate sodium was from Biomol (Plymouth Meeting, PA, USA), and iberiotoxin was from Alomone Labs (Jerusalem, Israel). α-Bungarotoxin was kindly provided by Dr. Long-Seng Chang, Institute of Biomedical Sciences, National Sun Yat-sen University, Kaohsiung City, Taiwan. Tissue culture media and trypsin/EDTA were obtained from American Type Culture Collection. L-glutamine, penicillin-streptomycin and fungizone were obtained from Life Technologies. All other chemicals were commercially available and of reagent grade.

The composition of normal Tyrode's solution was 136.5 mM NaCl, 5.4 mM KCl, 1.8 mM $CaCl_2$, 0.53 mM $MgCl_2$, 5.5 mM D-glucose, and 5.5 mM HEPES-NaOH buffer, pH 7.4. To record K^+ currents or membrane potential, the patch pipette was filled with a solution consisting of 140 mM KCl, 1 mM $MgCl_2$, 3 mM Na_2ATP, 0.1 mM Na_2GTP, 0.1 mM EGTA, and 5 mM HEPES-KOH buffer, pH 7.2. To measure Na^+ current, K^+ ions inside the pipette solution were replaced with equimolar Cs^+ ions, and the pH was adjusted to 7.2 with CsOH.

2.5. Computer simulation

To mimic the effects of ACO on spontaneous action potentials in differentiated NG108-15 neuronal cells, a cell model, originally described in gonadotropin-releasing hormone-secreting neurons (Van Goor et al., 2000), was modified and simulated. The basic model primarily consists of a Na^+ current, L- and T-type Ca^{2+} currents, and a delayed rectifier K^+ current, and an M-type current. In addition, *erg* (*ether-à-go-go*-related-gene) K^+ current was incorporated to this model, given that it was functionally present in these cells (Meves et al., 1999; Lo et al., 2003). Simulations were performed using the stochastic Euler algorithm as implemented in the program *xpp* with the aid of the X-Win32 version of XPPAUT on a Hewlett Packard (HP xw9300) Workstation (Palo Alto, CA) (Ermentrout, 2002; Wu and Chang, 2006). Expressions and parameters for ion currents, equilibrium functions, and parameter values are modified in this study. In the present simulations, the conductance values and reversal potentials, together with other parameters, used to solve the set of differential equations, are listed in Table 1. The integration algorithm is Cvode with a tolerance of 10^{-4} and a minimum time step of 10^{-4} s.

To model ACO-induced block of $I_{K(DR)}$ in these cells, a kinetic scheme similar to that described by Marom and Abbott (1994) was used in our study. Based on this formula, an inactivation variable $h2$ was incorporated into simulated $I_{K(DR)}$ and the macroscopic current was expressed as

$$I_{K(DR)} = G_K \times n(V)^4 \times h1(V) \times h2 \times (V - V_K).$$

Here, G_K is the maximal conductance of $I_{K(DR)}$, and V_K the K^+ reversal potential. However, as ACO-induced block is a state-dependent rather than voltage-dependent process, the form of the equation describing the inactivation variables was modified as follows:

$$\frac{dh_2}{dt} = k_1 \times (1 - h2) - k_{-1} \times n^4 \times h2,$$

Table 1
Default parameter values used for the modeling of differentiated NG108-15 neuronal cells

Symbol	Description	Value
Cm	Membrane capacitance	14.0 nF
g_{Na}	Na^+ current conductance	60 nS
$g_{Ca,L}$	L-type Ca^{2+} current conductance	1.1 nS
$g_{Ca,T}$	T-type Ca^{2+} current conductance	0.9 nS
$g_{K(DR)}$	Delayed rectifier K^+ current conductance	20 nS
g_M	M-type K^+ current conductance	4.0 nS
$g_{K(erg)}$	*erg*-like K^+ current conductance[a]	50 nS
V_{Na}	Na^+ reversal potential	60 mV
V_{Ca}	Ca^{2+} reversal potential	100 mV
V_K	K^+ reversal potential	−75 mV

[a] *erg*: *ether-à-go-go*-related-gene.

where k_1 and k_{-1} are voltage-independent rate constants for block and unblock by ACO. The equations used in the simulation for $I_{K(DR)}$ in differentiated NG108-15 cells, originally from the model of Van Goor et al. (2000), were:

$$n_\infty = \frac{1}{1 + \exp(-(25 + V)/15)},$$

$$\tau_n = 1 + \frac{15}{\exp((30 + V)/15)} + \exp(-(30 + V)/15),$$

$$\alpha h1_\infty = 0.3 + \frac{0.7}{1.0 + \exp(-(35 + V)/10)},$$

$$\tau_{h1} = 1000.$$

Source files used in this study can be available at http://senselab.med.yale.edu/senselab/modeldb.

3. Results

3.1. Effect of ACO on delayed rectifier K^+ current ($I_{K(DR)}$) in differentiated NG108-15 cells

The whole-cell configuration of the patch-clamp technique was used to evaluate the effect of ACO on ion currents in NG108-15 cells preincubated with dibutyryl cyclic AMP (1 mM). To record K^+ outward currents, cells were bathed in Ca^{2+}-free Tyrode's solution containing tetrodotoxin (1 μM) and $CdCl_2$ (0.5 mM). When the cell was held at −50 mV, depolarizing voltage pulses from −50 to +50 mV in 20-mV increments were applied with a duration of 1 s a family of large K^+ outward currents with little inactivation was elicited (Fig. 1). These outward currents have been previously identified as $I_{K(DR)}$ (Yokoyama et al., 1989; Wu et al., 2001; Tsai et al., 2006). When cells were exposed to ACO (10 μM), the amplitude of $I_{K(DR)}$ measured at the end of the voltage pulses was reduced at the potentials ranging from 0 to +50 mV. For example, when depolarizing pulses from −50 to +30 mV were applied, ACO (10 μM) significantly decreased current amplitude at the end of the voltage pulses from 998 ± 193 to 282 ± 58 pA ($n = 8$, $P < 0.05$). After washout, the amplitude of $I_{K(DR)}$ at +30 mV was partially returned to 852 ± 95 pA ($n = 6$).

A dramatic change in the time course of $I_{K(DR)}$ was detected during the exposure to ACO (Fig. 1). After application of 10 μM ACO, outward currents activated to a maximum, and subsequently decayed over time, although no significant change was seen in the early activation kinetics of these currents (i.e., dI/dt). In addition, the peak amplitudes of $I_{K(DR)}$ were almost unaffected in the presence of 1 μM ACO. Averaged $I-V$ relations for the amplitude of initial and steady-state components of $I_{K(DR)}$ in the absence and presence of ACO (10 μM) are shown in Fig. 1B. These results indicate that ACO can suppress the amplitude of $I_{K(DR)}$ in a time-dependent fashion in differentiated NG108-15 cells.

The percentage inhibition of $I_{K(DR)}$ by ACO was also measured at test potentials between 0 and +50 mV. As shown in Fig. 1C, we found no significant difference in the percentage inhibition of ACO (10 μM) on $I_{K(DR)}$ across the voltages examined. For example, at a test potential of 0 mV, current was inhibited by 18 ± 6% ($n = 6$), while at +30 mV, inhibition was 22 ± 7% ($n = 6$). Thus, these results suggest that

Please cite this article in press as: Lin, M.-W. et al., Characterization of aconitine-induced block of delayed rectifier K^+ current in differentiated NG108-15 neuronal cells, Neuropharmacology (2008), doi:10.1016/j.neuropharm.2008.01.009

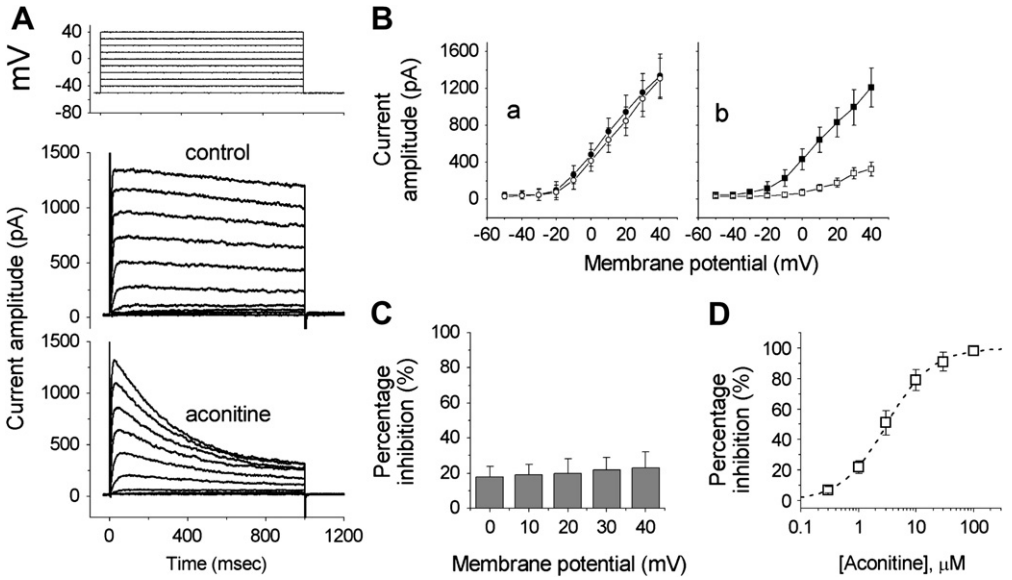

Fig. 1. Inhibitory effect of ACO on $I_{K(DR)}$ in differentiated NG108-15 cells. Cells were bathed in Ca^{2+}-free Tyrode's solution containing tetrodotoxin (1 μM) and $CdCl_2$ (0.5 mM). (A) Superimposed current traces in the absence and presence of ACO (1 μM). The cell was depolarized from −50 mV to various potentials ranging from −50 to +50 mV in 20-mV increments. Current traces shown on the upper part are control, and those on the lower part were obtained 2 min after addition of ACO (10 μM). (B) Averaged I–V relations for initial (Ba) and steady-state (Bb) components of $I_{K(DR)}$ in the absence (filled symbols) and presence (open symbols) of 10 μM ACO. Mean ± SEM ($n = 6$–11). (C) Bar graph showing little or no voltage-dependence for ACO-induced block of $I_{K(DR)}$. The percentage inhibition of $I_{K(DR)}$ by ACO (1 μM) was shown over the voltage range of 0 to +50 mV (mean ± SEM, $n = 5$–10). (D) Concentration-response curve for ACO-induced inhibition of $I_{K(DR)}$. The amplitude of $I_{K(DR)}$ during the exposure to ACO was compared with the control value, i.e., in the absence of ACO (mean ± SEM, $n = 4$–9 for each point). The smooth line represents the best fit to a Hill function. The values for IC_{50}, maximally inhibited percentage of $I_{K(DR)}$ and the Hill coefficient were 3.1 μM, 100% and 1.1, respectively.

block by ACO of $I_{K(DR)}$ in NG108-15 cells shows little or no voltage-dependence, although a time-dependent block can be clearly observed.

Fig. 1D shows the relationship between the concentration of ACO and the percentage inhibition of $I_{K(DR)}$. In these experiments, each cell was depolarized from −50 to +50 mV with a duration of 1 s. Current amplitudes were measured at the end of depolarizing pulses. ACO (0.3–100 μM) suppressed the steady-state component of $I_{K(DR)}$ in a concentration-dependent manner. With the use of a non-linear least-squares fit of the data, the half-maximal concentration (i.e., IC_{50}) required for the inhibitory effect of ACO on $I_{K(DR)}$ was calculated to be 3.1 μM, and at a concentration of 100 μM, it almost completely suppressed the steady-state component of $I_{K(DR)}$. Thus, it is apparent that ACO can exert a significant action on the inhibition of $I_{K(DR)}$ in differentiated NG108-15 cells.

3.2. $I_{K(DR)}$ recovery from block in the presence of ACO

Recovery from block was further determined using a double-pulse protocol consisting of a first (conditioning) depolarizing pulse sufficiently long to allow block to reach a steady-state. During the exposure to ACO (3 μM), the membrane potential was then stepped to +50 mV from −50 mV for a variable time, after which a second depolarizing pulse (test pulse) was applied at the same potential as the conditioning pulse (Fig. 2). The ratios of the peak current amplitudes of $I_{K(DR)}$ evoked in response to the test and the conditioning pulse were then taken as a measure of recovery from block, and plotted versus interpulse interval. Recovery was generally complete, and its time course described by a single exponential with a time constant of 2.56 ± 0.17 s ($n = 5$). When cells were exposed to 10 μM ACO, no change in the mean time constant (2.63 ± 0.31 s) for recovery from inactivation was seen. Thus, recovery of $I_{K(DR)}$ was not affected by ACO.

3.3. Effect of ACO on steady-state inactivation of $I_{K(DR)}$

The effect of ACO on the steady-state inactivation of $I_{K(DR)}$ in NG108-15 cells was also evaluated and the experimental

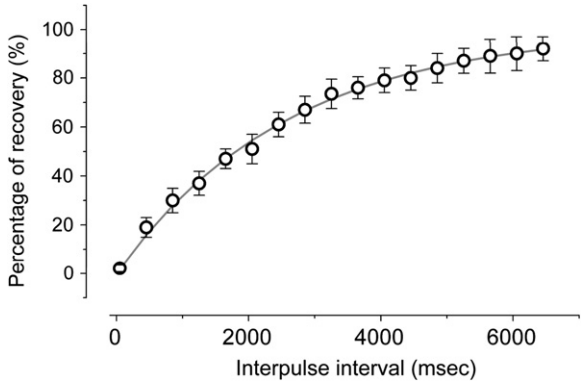

Fig. 2. Time course of the recovery of $I_{K(DR)}$ in the presence of 3 μM ACO. Cells, bathed in Ca^{2+}-free Tyrode's solution, were depolarized from −50 to +50 mV with a duration of 1 s and different interpulse durations were applied. The time course as indicated in smooth line was well fitted to a single exponential with a time constant of 2.56 s. Each point represents mean ± SEM ($n = 4$–7).

Please cite this article in press as: Lin, M.-W. et al., Characterization of aconitine-induced block of delayed rectifier K^+ current in differentiated NG108-15 neuronal cells, Neuropharmacology (2008), doi:10.1016/j.neuropharm.2008.01.009

data are shown in Fig. 3. In this series of experiments, cells were bathed in Ca^{2+}-free, Tyrode's solution and the steady-state inactivation parameters of $I_{K(DR)}$ were obtained in the absence and presence of ACO (10 μM) under the aid of another double-pulse protocol (Fig. 3). In Fig. 3B, the normalized amplitude of $I_{K(DR)}$ (i.e., I/I_{max}) was constructed against the conditioning potential and the curves were fitted by a Boltzmann function using least-squares method:

$$I = \frac{I_{max}}{1 + \exp[(V - a)/b]},$$

where I_{max} is the maximal activated $I_{K(DR)}$, V is the membrane potential in mV, a is the membrane potential for half-maximal inactivation, and b is the slope factor of the inactivation curve. In the absence of ACO, $a = -15.1 \pm 1.2$ mV and $b = 4.5 \pm 0.2$ mV ($n = 5$), whereas in the presence of ACO (10 μM), $a = -37.2 \pm 1.6$ mV, $b = 4.6 \pm 0.3$ mV ($n = 5$). ACO (10 μM) could thus shift the midpoint of the inactivation curve toward hyperpolarizing voltage by approximately 22 mV, although no change in the slope factor (i.e., b) was detected in the presence of ACO. Thus, there was voltage-dependence of the steady-state inactivation curve of $I_{K(DR)}$ in the presence of ACO.

3.4. ACO-induced increase in cumulative inhibition of $I_{K(DR)}$ inactivation

$I_{K(DR)}$ inactivation accumulated during repetitive short pulses as described previously (Marom et al., 1993). In other words, inactivation obtained during a train of short pulses became drastically faster than that in response to a single maintained pulse of the same duration. Thus, in the next series of experiments, we sought to determine whether ACO affects the change in the time course of $I_{K(DR)}$ inactivation in differentiated NG108-15 cells. Under control conditions, a single 20-s depolarizing step to +80 mV from −90 mV produced a decline with a time constant of 6.6 ± 0.2 s ($n = 7$). However, the time constant for 20-s repetitive pulses to +80 mV, each of which lasted 40 ms with 20-ms intervals at −40 mV between the depolarizing pulses, was significantly reduced to 2.4 ± 0.1 s ($n = 6$, $P < 0.05$). The results indicates a progressive increase in the decline of $I_{K(DR)}$ in response to rapid depolarizing stimuli as reported previously (Marom et al., 1993). During the exposure to 1 μM ACO, the value of time constant obtained during this train of short repetitive pulses was further decreased to 1.1 ± 0.1 s ($n = 6$, $P < 0.05$). A representative example of cumulative inhibition of $I_{K(DR)}$ inactivation with or without application of ACO is illustrated in Fig. 4.

3.5. Kinetic studies of ACO-induced block of $I_{K(DR)}$

Because in the presence of ACO, $I_{K(DR)}$ exhibited a pronounced peak followed by an exponential decay to a steady-state level, it is thus important to determine the kinetics of ACO-induced block of $I_{K(DR)}$. The concentration-dependence of $I_{K(DR)}$ decay by ACO is illustrated in Fig. 5. Although the initial activation phase of $I_{K(DR)}$ was unchanged during the exposure to ACO, its effects on $I_{K(DR)}$ were found to be a concentration-dependent increase in the rate of current decay accompanied by a decrease in the residual, steady-state current. In other words, increasing the concentration of ACO not only reduced the peak current, but also enhanced the apparent inactivation. Therefore, the inhibitory effect of ACO on $I_{K(DR)}$ in NG108-15 cells can be explained by state-dependent block where it binds to the open state of the channel according to the minimal kinetic scheme:

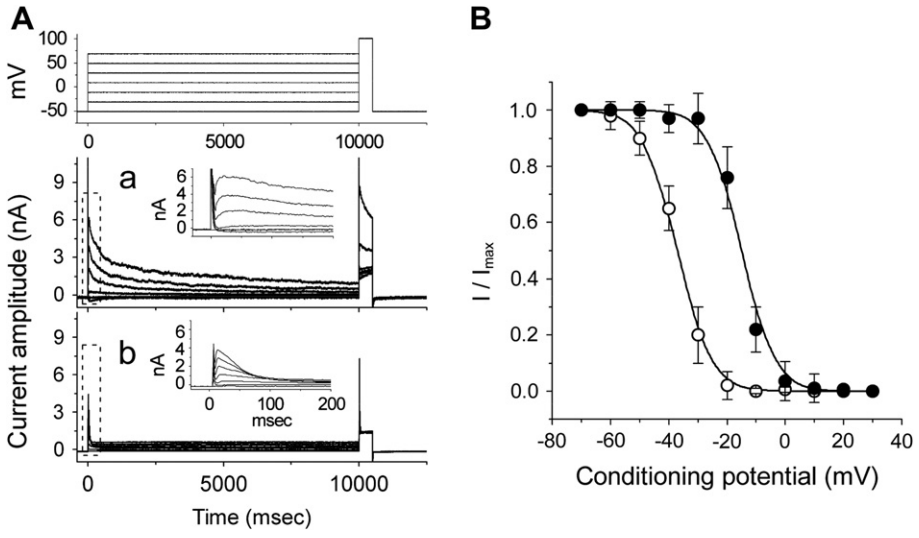

Fig. 3. Effect of ACO on steady-state inactivation of $I_{K(DR)}$ in differentiated NG108-15 cells. (A) Superimposed current traces obtained in the absence (a) and presence (b) of 10 μM ACO. The conditioning voltage pulses with a duration of 10 s to various membrane potentials ranging from −50 to +70 mV in 20-mV increments were applied from a holding potential of −50 mV. Following each conditioning pulse, a test pulse to +100 mV with a duration of 500 ms was applied to elicit $I_{K(DR)}$. Upper part indicates the voltage protocol used. Insets indicate expanded time scale of current traces (dashed boxes). (B) Steady-state inactivation of $I_{K(DR)}$ in the absence (●) and presence (○) of 10 μM ACO. Mean ± SEM ($n = 4$–7).

Please cite this article in press as: Lin, M.-W. et al., Characterization of aconitine-induced block of delayed rectifier K^+ current in differentiated NG108-15 neuronal cells, Neuropharmacology (2008), doi:10.1016/j.neuropharm.2008.01.009

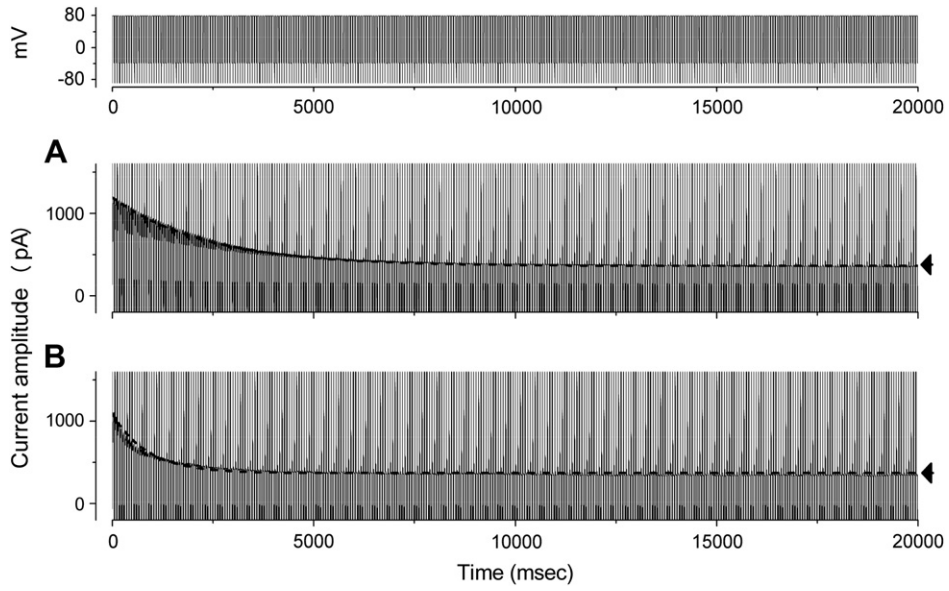

Fig. 4. Excessive accumulative inactivation of $I_{K(DR)}$ during repetitive stimuli in absence and presence of ACO recorded from differentiated NG108-15 cells. Currents were obtained during repetitive depolarizations to +80 mV, with return to −40 mV. The depolarizing pulses used to elicit outward currents lasted 40 ms. Current traces were obtained during a 20-s maintained depolarization pulse from −90 to +80 mV in the control (A) and during the exposure to 1 μM ACO (B). The upper part indicates the voltage protocol used. Dashed smooth curves in (A) and (B) indicated by arrowheads show the single-exponential fits with time constants of 2.4, and 1.1 s, respectively. Notably, in addition to the inhibition of $I_{K(DR)}$ amplitude, ACO increases the rate of excessive accumulative inactivation of $I_{K(DR)}$ evoked by repetitive stimuli.

$$C \underset{\beta}{\overset{\alpha}{\rightleftarrows}} O \underset{k_{-1}}{\overset{k_{+1}}{\rightleftarrows}} O \cdot B,$$

where α and β are the voltage-dependent rate constants for the opening and closing of the K_{DR} channel, k_{+1} and k_{-1}, those for block and unblock by ACO, and $[B]$ is the blocker (i.e., ACO) concentration. C, O and $O \cdot B$ are the closed, open, and open-blocked states, respectively.

Block and unblock rate constants, k_{+1} and k_{-1}, were determined from the time constants of current decay evoked by the depolarizing pulses (Fig. 5). Block and unblock rate constants could be estimated using the relation

$$\frac{1}{\tau_b} = k_{+1} \times [B] + k_{-1}.$$

In particular, k_{+1} and k_{-1}, respectively, result from the slope and from the y-axis intercept at $[B] = 0$ of the linear regression interpolating the reciprocal time constants (i.e., $1/\tau_b$) versus different ACO concentrations. As predicted by a first order blocking scheme, the relationship between $1/\tau_b$ and $[B]$ was linear with a correlation coefficient of 0.95 (Fig. 5B), and the block and unblock rate constants obtained from 6 to 11 different cells were calculated to be 0.00111 ms^{-1} μM^{-1} and 0.00132 ms^{-1}, respectively. Based on these rate constants, a value of 1.2 μM for the dissociation constant ($K_D = k_{-1}/k_{+1}$) could be derived. Notably, this value was noted to agree with the IC_{50} value determined from the concentration-response curve (Fig. 1D). However, the rate constant of the inverse reaction (i.e., unblock rate constant), k_{-1}, showed little dependence on $[B]$; k_{-1} was 0.00133 ± 0.002 ms^{-1} ($n = 5$) at 1 μM and 0.00135 ± 0.003 ms^{-1} ($n = 5$) at 3 μM.

To quantitatively analyze the effects of ACO on $I_{K(DR)}$ in NG108-15 cells, a mathematical model originally designed by Marom and Abbott (1994) was further implemented. As shown in Section 2, an inactivation model that is a voltage-independent but state-dependent process was incorporated to the kinetic scheme. A quantitative description of the $I_{K(DR)}$ in the absence and presence of different concentrations of ACO was then provided. Based on the rate constants determined from the fitting (Fig. 5B), simulated $I_{K(DR)}$ in the presence of different ACO concentrations were also obtained. Fig. 5C illustrates the results of simulated $I_{K(DR)}$ evoked in response to a test potential to +50 mV from −50 mV with a duration of 300 ms in the absence and in the presence of different ACO concentrations (1, 3, and 10 μM). The smooth lines indicate convincing fits to the experimental results when numerical parameters were appropriately chosen. These simulation profiles thus duplicate the experimental data and supports the notion that a concentration-dependent increase by ACO in the rate of inactivation can account for its reduction of $I_{K(DR)}$ in differentiated NG108-15 cells.

3.6. Inhibitory effect of ACO on voltage-dependent Na^+ current (I_{Na}) in differentiated NG108-15 cells

ACO has been recognized to exert effects on I_{Na} (Ameri, 1998; Wright, 2001; Wang and Wang, 2003). Moreover, there was an increase in the expression levels of $Na_v1.7$ in NG108-15 cells when neuronal differentiation was induced by pretreatment with a cyclic AMP analogue (Kawaguchi et al., 2007). The effect of ACO on I_{Na} was further investigated in this study. The experiments were conducted with a Cs^+-containing pipette

Please cite this article in press as: Lin, M.-W. et al., Characterization of aconitine-induced block of delayed rectifier K^+ current in differentiated NG108-15 neuronal cells, Neuropharmacology (2008), doi:10.1016/j.neuropharm.2008.01.009

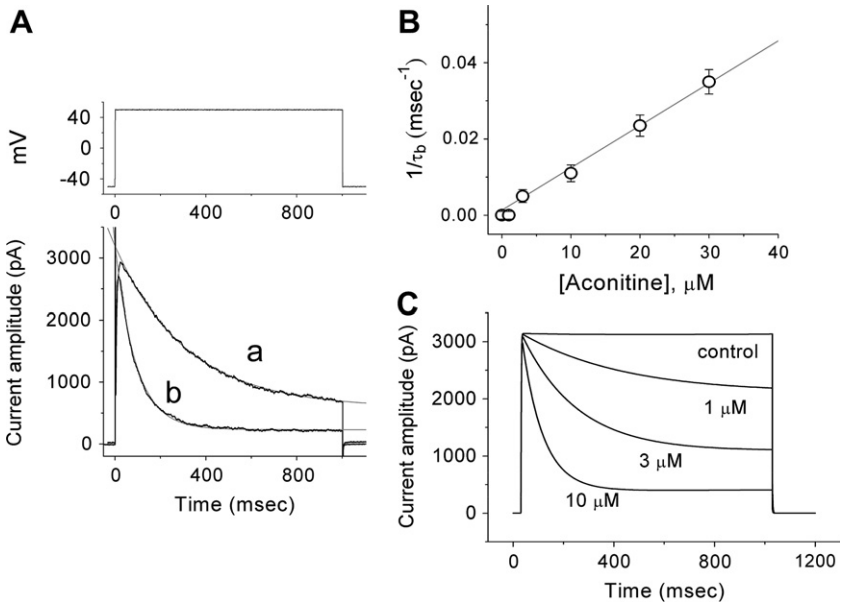

Fig. 5. Evaluation of the kinetics of ACO-induced block (A and B) and simulations of $I_{K(DR)}$ in the presence of different concentrations of ACO (C). In (A), typical $I_{K(DR)}$ was elicited by depolarizing pulses to +50 mV in the presence of ACO in the bath. The time courses of current decay in the presence of 3 and 10 μM ACO with a duration of 1 s were well fitted by a single exponential with a value of 308 and 82 ms, respectively. The upper part indicates the voltage protocol used. a: 3 μM ACO; b: 10 μM ACO. In (B), the reciprocal of the time constant of the rate of block, obtained by a single-exponential fit of the decay phase of $I_{K(DR)}$, was plotted against the ACO concentration. Data points were fitted by a linear regression, indicating that block occurs with a molecularity of 1. Block (k_{+1}) and unblock (k_{-1}) rate constants, given by the slope and the *y*-axis intercept of the interpolated line, were 0.00111 ms^{-1} μM^{-1} and 0.00132 ms^{-1}, respectively. Each point represents mean ± SEM ($n = 6–9$). In (C), the control trace was simulated with the assumption of typical values for $I_{K(DR)}$ in response to the depolarizing pulse from −50 to +50 mV. For simulated currents in the presence of ACO, the unblocking rate constant, k_{-1}, was fixed at 0.00132 ms^{-1} and the blocking rate constant, k_{+1} was expressed as the product of 0.00111 and the concentration of ACO in μM. The values shown at each current trace in (C) indicate the concentration of ACO mimicked.

solution. Each cell was held at the level of −80 mV and different depolarizing pulses (50 ms in duration) were delivered at a rate of 0.1 Hz. As shown in Fig. 6A, when the cell was depolarized from −80 to −20 mV, application of ACO (10 μM) significantly decreased the peak amplitude of I_{Na} from 2.04 ± 0.19 to 1.44 ± 0.13 pA ($n = 7$, $P < 0.05$). However, no change in the $I–V$ relationship of I_{Na} was detected in the presence of ACO (Fig. 6B). Thus, the results indicate that in differentiated NG108-15 cells, ACO produces a depressant action on I_{Na}.

The conductance-voltage relationship in the absence and presence of ACO was also compared and constructed. The data were fitted to Boltzmann function similar to that used for the inactivation curve of $I_{K(DR)}$ shown above. The results showed that although a significance decrease in maximal conductance of I_{Na} was found, half-maximal activation was not changed (Fig. 6C). However, based on the steady-state inactivation of I_{Na}, ACO (10 μM) can shift the midpoint of inactivation curve toward hyperpolarizing voltage by approximately 12 mV with no change in the slope factor (Fig. 6D).

3.7. Effect of ACO on repetitive firing of action potentials in differentiated NG108-15 cells

In another series of experiments, the effect of ACO on repetitive firing of action potentials was investigated in these cells. Cells were bathed in normal Tyrode's solution containing 1.8 mM $CaCl_2$, and current-clamp configuration was made with a K^+-containing pipette solution. A representative example of ACO-induced effects on spontaneous action potentials in these cells is illustrated in Fig. 7. When cells were exposed to ACO, the repetitive firing of action potentials was increased, along with increased widening of action potentials. For example, ACO at a concentration of 3 μM significantly increased the frequency from 0.37 ± 0.03 to 0.53 ± 0.04 Hz ($n = 5$, $P < 0.05$). The duration of action potentials was significantly prolonged to 345 ± 27 ms from a control value of 143 ± 18 ms ($n = 5$, $P < 0.05$). The ACO-induced changes in the firing of action potentials observed in these cells could be primarily explained by its block of $I_{K(DR)}$ and I_{Na}.

3.8. Effects of ACO on spontaneous action potentials in a modeled NG108-15 cell

In order to determine how ACO alters the discharge pattern of these cells, a simulation model, originally derived from Van Goor et al. (2000), was implemented (Fig. 8). In this modeled cell, as the I_{Na} conductance was decreased from 60 to 50 nS and the block of $I_{K(DR)}$ by ACO at a concentration of 3 μM was simulated, the firing and width of simulated action potentials was readily increased, along with the decrease in spike amplitude (Fig. 8A). When the I_{Na} conductance was further decreased to 40 nS and the ACO concentration was increased to 10 μM, the amplitude of action potentials was further reduced, together with prolonged action potential duration

Please cite this article in press as: Lin, M.-W. et al., Characterization of aconitine-induced block of delayed rectifier K^+ current in differentiated NG108-15 neuronal cells, Neuropharmacology (2008), doi:10.1016/j.neuropharm.2008.01.009

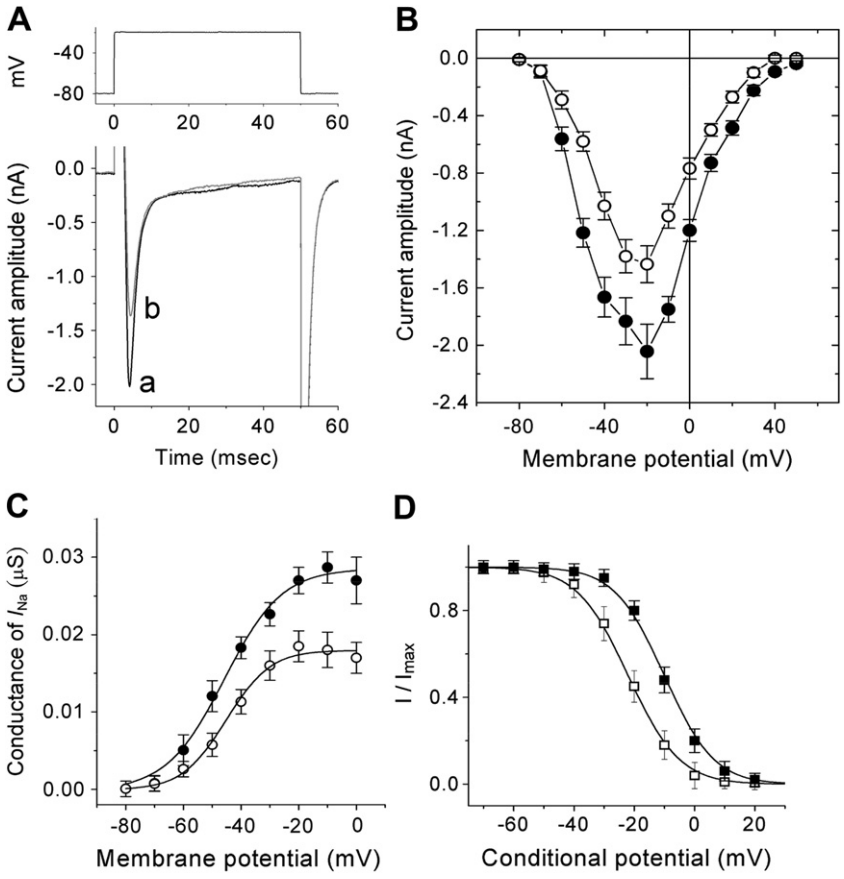

Fig. 6. Inhibitory effect of ACO on voltage-gated Na^+ current (I_{Na}) in differentiated NG108-15 cells. In these experiments, each pipette was loaded with a Cs^+-containing solution, and cells were bathed in normal Tyrode's solution containing 1.8 mM $CaCl_2$ and 10 mM tetraethylammonium chloride. The cell was depolarized from −80 mV to various potentials with a duration of 50 ms at a rate of 0.1 Hz. (A) Original current traces obtained in response to the depolarizing pulses from −80 to −20 mV. (a) control; (b) ACO (10 μM). The upper part in (A) indicates the voltage protocol used. (B) Averaged I–V relationships of I_{Na} in control (●) and during exposure to 10 μM ACO (○). Mean ± SEM ($n = 6$–9). (C) Conductance-voltage relationship of I_{Na} in the absence (●) and presence (○) of 10 μM ACO. (Mean ± SEM, $n = 5$–7). (D) Effect of ACO on steady-state inactivation of I_{Na} in differentiated NG108-15 cells. In these experiments, following each conditioning pulse, a test pulse to −20 mV with a duration of 50 ms was applied to elicit I_{Na}. ■: control; □: 10 μM ACO. (Mean ± SEM, $n = 4$–7).

(Fig. 8C). As a result, consistent with experimental results, the reduced I_{Na} and the increased decay of $I_{K(DR)}$ inactivation, which mimics the ACO action, can act combine to cause changes in the firing of simulated action potentials.

3.9. Effect of ACO on $I_{K(DR)}$ in differentiated SH-SY5Y neuronal cells

Finally, to verify whether the ACO-induced inhibition of $I_{K(DR)}$ could also be observed in another type of neuronal cells, we also investigated the effects of this compound on differentiated SH-SY5Y cells. As shown in Fig. 9, ACO (3 μM) significantly decreased the amplitude of $I_{K(DR)}$ measured at the end of depolarizing pulses by 54 ± 9% ($n = 5$). Block of $I_{K(DR)}$ by ACO was not instantaneous, but developed with time after the channels were opened, thus producing an apparent inactivation of the current. Consistent with the observations in NG108-15 cells, these data thus indicate that this alkaloid can induce the block of $I_{K(DR)}$ as well as accelerate current decay in SH-SY5Y cells.

4. Discussion

This study demonstrated that in differentiated NG108-15 neuronal cells, ACO, which is a toxic alkaloid (Lowe et al., 2005), induced a time-, concentration-, and state-dependent decay of $I_{K(DR)}$, without altering activation kinetics of this current. These observations, together with the good description of $I_{K(DR)}$ time course at different ACO concentrations with the computer simulation of the binding scheme, indicate that ACO may act as a state-dependent blocker. Block by ACO of $I_{K(DR)}$ is of importance because it may have characteristics that make it significant from a pharmacological point of view.

An important feature of the block of $I_{K(DR)}$ by ACO in NG108-15 cells is that the initial rising phase of the current (i.e., the activation time course) was unaffected in the presence of ACO. At the beginning of the voltage pulse, dI/dt will be proportional to the number of channels available for activation. Our experimental results showing that dI/dt was unchanged during cell exposure to ACO, suggest that before channel activation, there should be the absence of any significant resting block of K_{DR} channels. Another interesting finding in this study is that ACO tended to accelerate $I_{K(DR)}$

Please cite this article in press as: Lin, M.-W. et al., Characterization of aconitine-induced block of delayed rectifier K^+ current in differentiated NG108-15 neuronal cells, Neuropharmacology (2008), doi:10.1016/j.neuropharm.2008.01.009

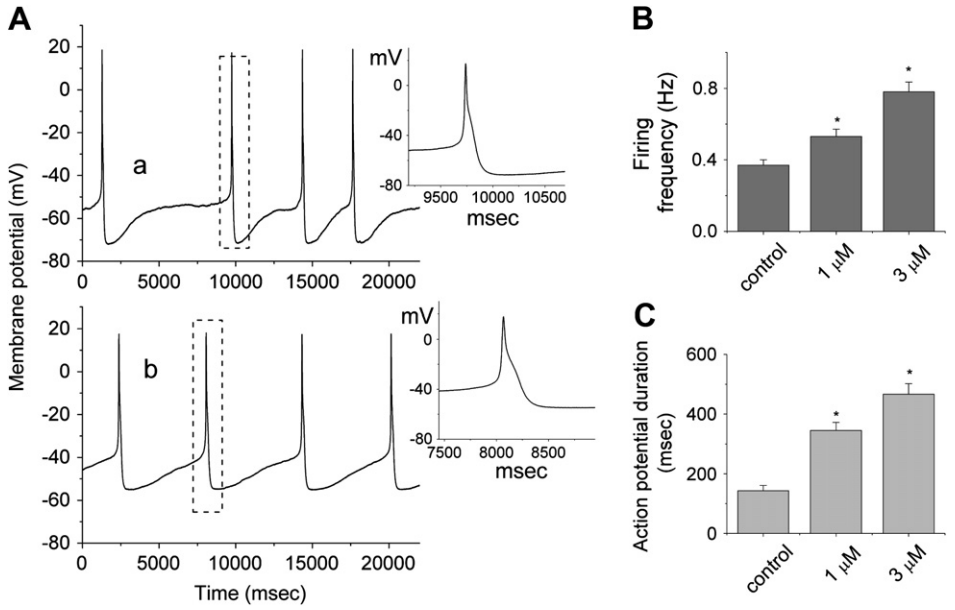

Fig. 7. Effect of ACO on the firing of action potentials in differentiated NG108-15 cells. Cells were bathed in normal Tyrode's solution containing 1.8 mM $CaCl_2$. Patch pipettes were filled with a K^+-containing solution. Membrane potential was measured under current-clamp configuration. (A) Original potential traces showing the effect of ACO on spontaneous action potentials. Trace a is the control, and traces b were obtained 2 min after application of 10 μM ACO. Inset shown in each trace represents the expanded record. (B) and (C) Bar graph in (B) and (C) illustrate the summary of the effect of ACO (1 and 3 μM) on the firing frequency and duration of action potentials, respectively. Each point represents the mean ± SEM ($n = 4–6$). *Significantly different from control ($P < 0.05$). Action potential duration was measured at 50% or repolarization.

inactivation, suggesting that the ACO molecule appears to reach the blocking site only when the channel is in the open state. This feature can thus be incorporated in the minimal binding scheme, i.e., closed ↔ open ↔ open-blocked (Wu et al., 2001). Inherent to this blocking scheme is that open-blocked channels are not closed unless ACO dissociates from the binding site, thus providing only one recovery path. Thus, based on modified Hodgkin and Huxley formalism

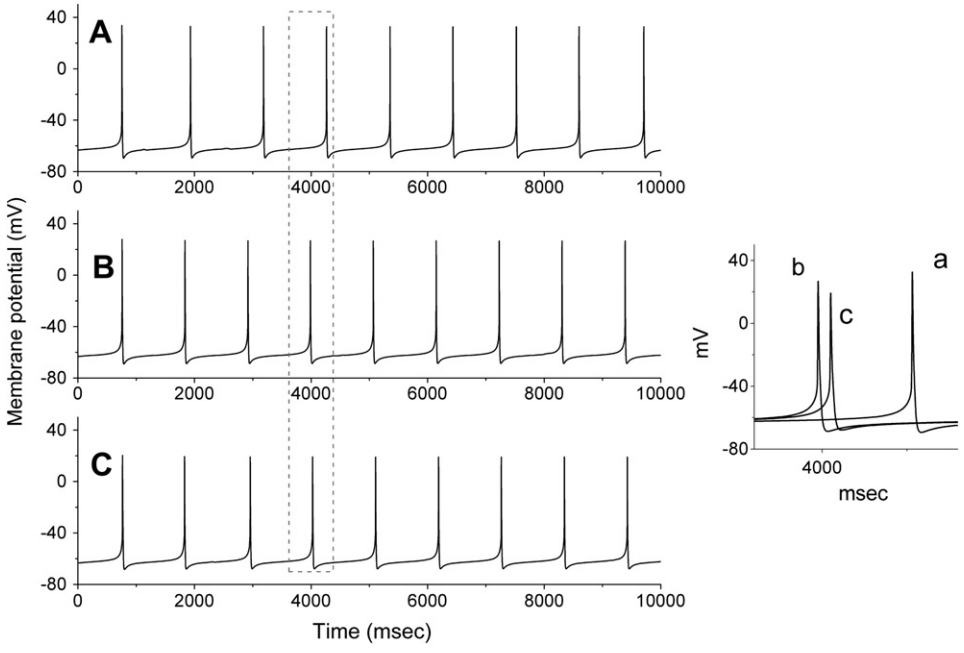

Fig. 8. Simulation modeling used to mimic ACO effects on repetitive firing of action potentials in NG108-15 neuronal cells. The model was developed based on the electrophysiological properties of gonadotropin-releasing hormone-secreting neurons as described in Section 2. In (A), the firing of spontaneous action potentials under control conditions is illustrated. In (B), when I_{Na} conductance was arbitrarily decreased from 60 to 50 nS and the ACO concentration was set at 3 μM, the peak amplitude of action potentials was readily reduced, together with the increase in the firing and duration of spike discharge. In (C), when I_{Na} conductance was decreased 40 nS in the continued presence of 10 μM ACO, the spike amplitude was further decreased, together with the increased width of action potentials in this modeled cell. The inset shown in the rightmost side indicates the expanded record. Potential traces labeled a, b and c corresponds to those in panel A, B and C (dashed box).

Please cite this article in press as: Lin, M.-W. et al., Characterization of aconitine-induced block of delayed rectifier K^+ current in differentiated NG108-15 neuronal cells, Neuropharmacology (2008), doi:10.1016/j.neuropharm.2008.01.009

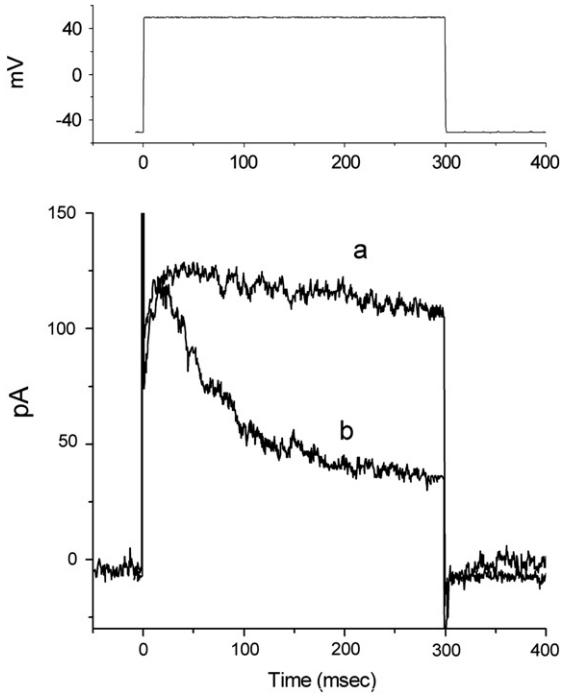

Fig. 9. Effects of ACO on $I_{K(DR)}$ in differentiated SH-SY5Y cells. Cells were bathed in Ca^{2+}-free Tyrode's solution. Whole-cell currents were evoked by 300-ms depolarizing pulses from −50 to +50 mV. Current traces labeled a and b indicate those obtained in the absence and presence of 3 μM ACO, respectively.

(Marom and Abbott, 1994), a kinetic scheme was also designed to describe ACO-induced block of $I_{K(IR)}$ in our study. ACO-induced block was thus interpreted to mean that it preferentially binds to and block an open state of the channel. This simulation model could duplicate the experimental results and was verified to be useful for evaluation of ACO-induced block on $I_{K(DR)}$ in NG108-15 cells. However, notably, ACO is also likely to be trapped in closed channels, thus leading to a slowing in recovery of $I_{K(DR)}$. Similar hyperpolarizing shift in the steady-state inactivation curve of $I_{K(DR)}$ shown in this study may be explained by a ''foot in the door'' mechanism in which a slowing in the deactivation of the channels can occur (Decher et al., 2006).

The observed effects of ACO on $I_{K(DR)}$ in NG108-15 cells clearly did not involve the suppression of Ca^{2+}-dependent K^+ channels or ATP-sensitive K^+ channels. All recordings of $I_{K(DR)}$ presented here were conducted in a Ca^{2+}-free Tyrode's solution containing $CdCl_2$ (0.5 mM). Furthermore, neither peak amplitudes nor inactivation kinetics of $I_{K(DR)}$ were altered by iberiotoxin or 5-hydroxydecanoate sodium. However, the blockade of $I_{K(DR)}$ by ACO can be primarily responsible for its actions on the broadening of action potentials in these cells, because it was not found to increase the amplitude of I_{Na}.

Previous reports showed the presence of cholinergic receptors in NG108-15 cells (Ling et al., 2005). ACO has been reported to be an antagonist of α7-selective nicotinic receptors (Hardick et al., 1995). One may thus expect that ACO-induced block of ion currents presented herein is associated with its inability to bind to nicotinic receptors. However, either orphenadrine (30 μM), an anticholinergic agents (Pubill et al., 2001), or methyllycaconitine (30 μM), an antagonist of α_7-nicotinic receptors (Hardick et al., 1995), slightly suppressed the amplitude of $I_{K(DR)}$ with no any changes in current inactivation in these cells. α-Bungarotoxin (1 μM), a blockers of α_7 nACh receptors (McGehee and Role, 1995), was found to have no effect on $I_{K(DR)}$. Therefore, our study showed that inhibitory effects of ACO on $I_{K(DR)}$ in NG108-15 cells did not appear to be mediated through the blockade of nicotinic receptors.

ACO may be an important tool for probing the structure and function of K^+ channels from the K_{DR} family, because the pore region of the channel protein to which it binds is of particular relevance for open-channel blockade. The role of K_{DR} channel particularly members of the Kv3 superfamily is to stabilize the resting membrane potential and reduce the width of high-frequency action potentials in time-coding neurons (Marom, 1998; Hernandez-Pineda et al., 1999; Rudy and McBain, 2001; Lien and Jonas, 2003; Tateno and Robinson, 2007). The block of K_{DR} channels by ACO, together with an increase in action potential duration, may be responsible for its effects on neuronal excitability. ACO-induced block of $I_{K(DR)}$ will even become very significant when a train of action potentials occurs, because of the fact that under these conditions, the availability of K_{DR} channels is decreased as a function of firing frequency (Marom et al., 1993; Rudy and McBain, 2001; Lien and Jonas, 2003).

Inactivation is a basic conformational change intrinsic to most of the K^+ channels that controls repolarization. Inactivation has been observed for many cloned K^+ channels of the K_v superfamily, and is generally termed ''C-type inactivation'', to contrast with ''N-type'' inactivation by the ''ball-and-chain'' mechanism (Baukrowitz and Yellen, 1995; Rasmusson et al., 1998; Fernandez et al., 2003). C-type inactivation, that has been reported to occur in Kv3 and Kv2 channels (Marom et al., 1993), was thought to involve a concerted constriction of the outer part of the channel pore. Moreover, in our study, because intracellular dialysis with 100 μM ACO did not affect the rate of $I_{K(DR)}$ inactivation, ACO induced block of $I_{K(DR)}$ in a time-dependent fashion possibly by acting at a site that is accessible from the extracellular side of the channel. ACO could enhance cumulative inhibition of $I_{K(DR)}$ inactivation. The steady-state inactivation curve of $I_{K(DR)}$ was shifted to a hyperpolarized potential in the presence of ACO. Therefore, ACO is likely to interact with the inactivated state of the K_{DR} channels. As onset of C-type inactivation was accelerated by ACO, there appears to be an interaction between the binding of ACO and C-type inactivation in differentiated NG108-15 cells. ACO and its structurally-related alkaloids may be the harbinger of new and more specifically acting compounds that use the C-inactivated state as a substrate.

In our study, ACO is a potent blocker of $I_{K(DR)}$ in NG108-15 or SH-SY5Y neuronal cells. The IC_{50} value of ACO required for the inhibition of $I_{K(DR)}$ was 3.4 μM. Because its effects shown here may occur at a concentration achievable in humans, the present findings suggest that the K_{DR} channel may be a target for the action of ACO. It is thus tempting to

Please cite this article in press as: Lin, M.-W. et al., Characterization of aconitine-induced block of delayed rectifier K^+ current in differentiated NG108-15 neuronal cells, Neuropharmacology (2008), doi:10.1016/j.neuropharm.2008.01.009

speculate that the sensitivity of neurons to this compound would depend on the level of resting membrane potential, the firing of action potentials, and the concentration of ACO, if the ACO action *in vivo* is the same as those presented here. Moreover, it remains to be determined whether this blocking action is related to ACO-induced facilitation of spontaneous transmitter release in hypothalamic neurons (Yamanaka et al., 2002). Effect of ACO on reconstituted pure Kv3.1 channels also remains to be further investigated.

Our results seem to be distinguishable from previous reports where they showed the stimulatory effect of ACO on I_{Na} (Ameri, 1998; Wright, 2001; Wang and Wang, 2003). This discrepancy is currently unknown. However, it could be due to the different variants of Na^+ channels, as $Na_v1.7$ was found to be a major subfamily of Na^+ channels functionally expressed in differentiated NG108-15 cells (Kawaguchi et al., 2007). Nonetheless, ACO-induced blockade of $I_{K(DR)}$ and I_{Na} may synergistically affect the functional activity of neurons. These effects may have pharmacological or toxicological significance (Ameri et al., 1996; Friese et al., 1997; Yamanaka et al., 2002; Fu et al., 2006).

Our simulation results also imply that both blockade of I_{Na} and $I_{K(DR)}$ caused by ACO may synergistically act to affect the functional activity of neurons or neuroendocrine cells. Taken together, in addition to the blockade of I_{Na}, our results lead us to suggest that ACO-mediated action could be partly associated with a direct inhibition of K_{DR} channels expressed in neurons *in vivo*.

Acknowledgements

The work was partly supported by grants from the National Science Council (NSC-93-2320B-006-055 and NSC-94-2320B-006-019), and the Program for Promoting Academic Excellence and Developing World Class Research Centers, Ministry of Education, Taiwan.

References

Ameri, A., 1998. The effects of *Aconitum* alkaloids on the central nervous system. Prog. Neurobiol. 1998 (56), 211–235.

Ameri, A., Shi, O., Aschoff, J., Peters, T., 1996. Electrophysiological effects of aconitine in rat hippocampal slices. Neuropharmacology 35, 13–22.

Amran, M.S., Hashimoto, K., Homma, N., 2004. Effects of sodium-calcium exchange inhibitors, KB-R7943 and SEA0400, on aconitine-induced arrhythmias in guinea pigs in vivo, in vitro, and in computer simulation studies. J. Pharmacol. Exp. Ther. 310, 83–89.

Baukrowitz, T., Yellen, G., 1995. Modulation of K^+ current by frequency and external $[K^+]$: a tale of two inactivation mechanisms. Neuron 15, 951–960.

Brown, D.A., Higashida, H., 1988. Voltage and calcium-activated potassium currents in mouse neuroblastoma X rat glioma hybrid cells. J. Physiol. 397, 149–165.

Decher, N., Kumar, P., Gonzalez, T., Pirard, B., Sanguinetti, M.C., 2006. Binding site of a novel Kv1.5 blocker: a ''foot in the door'' against atrial fibrillation. Mol. Pharmacol. 70, 1204–1211.

Ermentrout, G.B., 2002. Simulating, Analyzing, and Animating Dynamical System: A Guide to XPPAUT for Researchers and Students. Society for Industrial and Applied Mathematics. SIAM, Philadelphia.

Fernandez, F.R., Morales, E., Rashid, A.J., Dunn, R.J., Turner, R.W., 2003. Inactivation of Kv3.3 potassium channels in heterologous expression systems. J. Biol. Chem. 278, 40890–40898.

Friese, J., Gleitz, J., Gutser, U.T., Heubach, J.F., Matthiesen, T., Wilffert, B., Selve, N., 1997. *Aconitum* sp. alkaloids: the modulation of voltage-dependent Na^+ channels, toxicity and antinociceptive properties. Eur. J. Pharmacol. 337, 165–174.

Fu, M., Wu, M., Qiao, Y., Wang, Z., 2006. Toxicological mechanisms of Aconitum alkaloids. Pharmazie 61, 735–741.

Hardick, D.J., Cooper, G., Scott-Ward, T., Blagbrough, I.S., Potter, B.V., Wonnacott, S., 1995. Conversion of the sodium channel activator aconitine into a potent α7-selective nicotinic ligand. FEBS Lett. 365, 79–82.

Hernandez-Pineda, R., Chow, A., Amarillo, Y., Moreno, H., Saganich, M., de Miera, E.V., Hernandez-Cruz, A., Rudy, B., 1999. Kv3.1–Kv3.2 channels underlie a high-voltage-activating component of the delayed rectifier K^+ current in projecting neurons from the globus pallidus. J. Neurophysiol. 82, 1512–1528.

Kawaguchi, A., Asano, H., Matsushima, K., Wada, T., Yoshida, S., Ichida, S., 2007. Enhancement of sodium current in NG108-15 during neural differentiation is mainly due to an increase in $Na_v1.7$ expression. Neurochem. Res. 32, 1469–1475.

Klemic, K.G., Kirsch, G.E., Jones, S.W., 2001. U-type inactivation of Kv3.1 and Shaker potassium channels. Biophys. J. 81, 814–826.

Lien, C.C., Jonas, P., 2003. Kv3 potassium conductance is necessary and kinetically optimized for high-frequency action potential generation in hippocampal interneurons. J. Neurosci. 23, 2058–2068.

Ling, K.K., Siow, N.L., Choi, R.C., Tsim, K.W., 2005. ATP potentiates the formation of AChR aggregate in the co-culture of NG108-15 cells with C2C12 myotubes. FEBS Lett. 579, 2469–2474.

Lo, Y.K., Chiang, H.T., Wu, S.N., 2003. Effect of arvanil (N-arachidonoyl-vanillyl-amine), a nonpungent anandamide-capsaicin hybrid, on ion currents in NG108-15 neuronal cells. Biochem. Pharmacol. 65, 581–591.

Lowe, L., Matteucci, M.J., Schneir, A.B., 2005. Herbal aconite tea and refractory ventricular tachycardia. New. Engl. J. Med. 353, 1532.

Marom, S., 1998. Slow changes in the availability of voltage-gated ion channels: effects on the dynamics of excitable membranes. J. Membr. Biol. 161, 105–113.

Marom, S., Abbott, L.F., 1994. Modeling state-dependent inactivation of membrane currents. J. Membr. Biol. 67, 515–520.

Marom, S., Goldstein, S.A., Kupper, J., Levitan, I.B., 1993. Mechanism and modulation of inactivation of the Kv3 potassium channels. Receptors Channels 1, 81–88.

McGehee, D.S., Role, L.W., 1995. Physiological diversity of nicotinic acetylcholine receptors expressed by vertebrate neurons. Annu. Rev. Physiol. 57, 521–546.

Meves, H., Schwarz, J.R., Wulfsen, I., 1999. Separation of M-like current and ERG current in NG108-15 cells. Br. J. Pharmacol. 127, 1213–1223.

Pubill, D., Vergaguer, E., Canudas, A.M., Sureda, F.X., Escubedo, E., Camarasa, J., Pallàs, M., Camins, A., 2001. Orphenadrine prevents 3-nitropropionic acid-induced neurotoxicity in vitro and in vivo. Br. J. Pharmacol. 132, 693–702.

Rasmusson, R.L., Morales, M.J., Wang, S., Liu, S., Campbell, D.L., Brahmajothi, M.V., Strauss, H.C., 1998. Inactivation of voltage-gated cardiac K^+ channels. Circulation Res. 82, 739–750.

Rudy, B., McBain, C.J., 2001. Kv3 channels: voltage-gated K^+ channels designed for high-frequency repetitive firing. Trends Neurosci. 24, 517–526.

Tateno, T., Robinson, H.P., 2007. Quantifying noise-induced stability of a cortical fast-spiking cell model with Kv3-channel-like current. Biosystems 89, 110–116.

Tojima, T., Kobayashi, S., Ito, E., 2003. Dual role of cyclic AMP-dependent protein kinase in neuritogenesis and synaptogenesis during neuronal differentiation. J. Neurosci. Res. 74, 829–837.

Tsai, T.Y., Tsai, Y.C., Wu, S.N., Liu, Y.C., 2006. Tramadol-induced blockade of delayed rectifier potassium current in NG108-15 neuronal cells. Eur. J. Pain 10 (7), 597–601.

Please cite this article in press as: Lin, M.-W. et al., Characterization of aconitine-induced block of delayed rectifier K^+ current in differentiated NG108-15 neuronal cells, Neuropharmacology (2008), doi:10.1016/j.neuropharm.2008.01.009

Van Goor, F., LeBeau, A.P., Krsmanovic, L.Z., Sherman, A., Catt, K.J., Stojilkovic, S.S., 2000. Amplitude-dependent spike-broadening and enhanced Ca^{2+} signaling in GnRH-secreting neurons. Biophys. J. 79, 1310–1323.

Wang, S.Y., Wang, G.K., 2003. Voltage-gated sodium channels as primary targets of diverse lipid-soluble neurotoxins. Cell. Signal 15, 151–159.

Wright, S.N., 2001. Irreversible block of human heart (hH1) sodium channels by the plant alkaloid lappaconitine. Mol. Pharmacol. 59, 183–192.

Wu, S.N., Chang, H.D., 2006. Diethyl pyrocarbonate, a histidine-modifying agent, directly stimulates activity of ATP-sensitive potassium channels in pituitary GH_3 cells. Biochem. Pharmacol. 71, 615–623.

Wu, S.N., Lo, Y.K., Chen, H., Li, H.F., Chiang, H.T., 2001. Rutaecarpine-induced block of delayed rectifier K^+ current in NG108-15 neuronal cells. Neuropharmacology 41, 834–843.

Xu, H., Arita, H., Hayashida, M., Zhang, L., Sekiyama, H., Hanaoka, K., 2006. Pain-relieving effects of processed Aconiti tuber in CCI-neuropathic rats. J. Ethnopharmacol. 103, 392–397.

Yamanaka, H., Doi, A., Ishibashi, H., Akaike, N., 2002. Aconitine facilitates spontaneous transmitter release at rat ventromedial hypothalamic neurons. Br. J. Pharmacol. 135, 816–822.

Yokoyama, S., Imoto, K., Kawamura, T., Higashida, H., Iwabe, N., Miyata, T., Numa, S., 1989. Potassium channels from NG108-15 neuroblastoma-glioma hybrid cells. FEBS Lett. 259, 37–42.

Please cite this article in press as: Lin, M.-W. et al., Characterization of aconitine-induced block of delayed rectifier K^+ current in differentiated NG108-15 neuronal cells, Neuropharmacology (2008), doi:10.1016/j.neuropharm.2008.01.009